

Back-iron Consideration in High-Speed Axial-Flux Machine

M. Sadeghierad, H. Lesani, H. Monsef

*Faculty of Elec. & computer engineering, University of Tehran,
 Amir abad (North Kargar) Street, Tehran, Iran, phone: 0098-911-2496053, e-mail: msadeghierad@yahoo.com*

A. Darabi

*Faculty of Elec. & Robotic Engineering, Shahrood University of Tech.,
 Shahrood, Iran, phone: 0098-912-2731386, e-mail: darabi_ahmad@hotmail.com*

Introduction

Recently more attention is paid to the development of high speed PM generators driven by micro turbines [1–5]. Nevertheless, the high-speed operation imposes stringent engineering design constrains which are not considered in conventional machine [6, 7].

This paper is devoted to modeling and designing of a permanent magnet synchronous alternator with axial flux structure. The back iron used in the rotors of two ends is the main subject investigated in the paper.

In the axial flux machine, back iron of the rotor dose the same job that in conventional machine with some differences. The yoke of the stator of the conventional machine presents some iron loss increasing with frequency but in the axial flux machine, the back iron rotates with the rotors. This paper presents a full consideration and impact of the back iron of high speed axial flux generator (HSAFG) on the performance characteristics including voltage, output power and efficiency.

Design

Fig. 1 shows a schematic view of an axial flux machine with three rotors and two stators.

Due to the high speed of the rotor and high frequency of the stator flux variation, the design of a high-speed machine is quite different from designing a conventional low speed and low frequency machine [8–10].

Sintered Nd-Fe-B material is generally the best candidate for use in the rotor of the PM machines [11]. In addition, coreless stator is a common suggestion for axial flux machine due to high frequency stator current and flux [12–16].

For the modeling purposes, the magnetic circuit of the machine with all details is required. Simple magnetic circuit of the HSAEG machine comprising all reluctances is shown in Fig. 2. The leakage reluctances R_{l1} and R_{l2} and

fringing reluctance R_g are taking into account for most accuracy of the model. As an example, the air gap flux densities are 0.488 and 0.5617 Tesla when these parameters are taken into account or ignored respectively.

All the parameters of the magnetic circuit are calculated by design-based equations given in [17]. R_{L1} is the PM leakage reluctance and is equal to:

$$R_{L1} = R_A \parallel R_B, \quad (1)$$

$$R_A = \frac{2\left(\frac{P}{2}\right)}{\mu_0 \delta \left((D_i - L_{PM}) L_n \frac{L_{PM} + 2g}{L_{PM}} + 2g \right)}, \quad (2)$$

$$R_B = \frac{9\left(\frac{P}{2}\right)}{\mu_0 \delta \left((3D_o + 2L_{PM}) L_n \frac{L_{PM} + 3g}{L_{PM}} - 6g \right)}. \quad (3)$$

The reluctance for leakage flux occurred between two PMs is:

$$R_{L2} = \frac{1}{\mu_0 P e r_1}, \quad (4)$$

$$P e r_1 (\text{permiance}) = \frac{L_{PM} \times P}{2\pi(1-\delta)} L_n \frac{R_o}{R_i}. \quad (5)$$

Reluctance of the PM

$$R_{PM} = \frac{L_{PM}}{\mu_0 \mu_r A_{PM}}. \quad (6)$$

The reluctance of the air gap including the stator can be written as:

$$R_{g1} = \frac{(L_s + 2g)}{\mu_0 A_g}. \quad (7)$$

Then the fringing effect is evaluated and total value for R_g is obtained using R_{g1} .

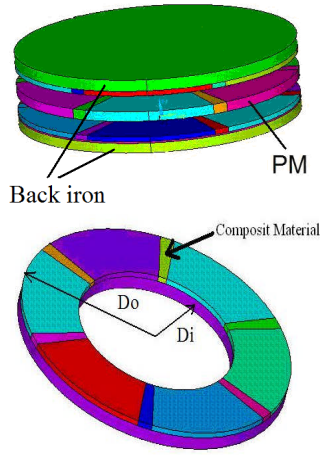


Fig. 1. View of a high-speed axial flux generator

For checking this Design, the FEM is used. The 2-D FE modeling of this machine can be carried out by introducing a radial cutting plane at the average radius, which is then developed into a 2-D flat model. The Neumann boundary condition is assigned to the top and bottom boundary. Result of 2D FEM (Magnetic Flux Density) is shown in Fig. 3.

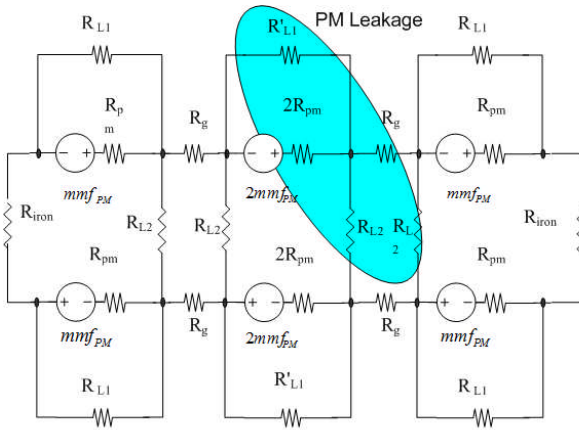


Fig. 2. Model of a Coreless HSAFG

List of symbols used in (1–7) and Fig. 1,2: μ_{air} – air viscosity coefficient (kg/ms); ρ – air density (kg/m³); g – air gap (m); L_{bi} – thickness of the back iron (m); L_{PM} – thickness of PM (m); L_s – thickness of stator (m); μ_0 – air magnetic permeability; μ_r – PM relative permeability; P – number of poles; δ – ratio of width of PM to pole pitch; P_{mech} – mechanical (windage) power loss (kW); P_{cu} – copper power loss (kW); P_{out} – output power (kW); P_{Loss} – power loss (kW); $P_{\text{eddy_Cu}}$ – eddy current power loss (kW); R_s – stator winding resistance (Ω); I_{load} – full load current of machine (A); B_g – air gap flux density (Tesla); N_m – rotor speed (rad/s); V_{cu} – volume of copper (winding) (m³); ρ_{cu} – electrical resistivity ($\Omega\cdot\text{m}$); N_s – number of series coil per phase; D_o – outer diameter (m); R_o – outer radius (m); D_i – inner diameter (m); R_i – inner radius (m); D_{sh} – shaft diameter (m); R_{sh} – shaft radius (m); D_{strand} – diameter of each conductor (m); A_g – area of air gap (m²); λ – ratio of D_i to D_o ($= \frac{1}{\sqrt{3}}$).

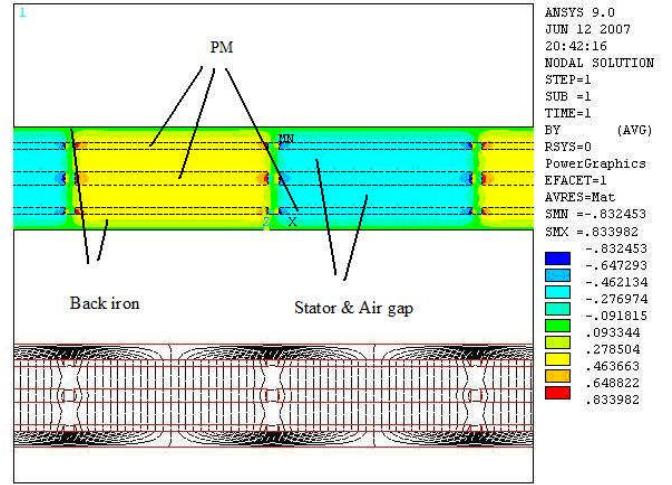


Fig. 3. An outline and a field analysis result of the machine by FEM

Loss calculation

In general heating is a main limitation of electrical machines but since the high temperature reduces magnetic quality of the permanent magnets therefore heating and high temperature relatively is much problematical in the PM machines. For this reason, loss calculation is important in the PM machines:

- Rotation losses were calculated using equation found in [18]. The power to overcome drag resistance of rotating disc is:

$$P_{\text{mech}} = \frac{1}{2} c_f \rho (2\pi N_m)^3 (R_o^5 - R_{sh}^5). \quad (8)$$

That C_f the coefficient of drag for turbulent flow can be found as

$$c_f = \frac{3.87}{\sqrt{\text{Re}}}. \quad (9)$$

That Re the Reynolds number for a rotating disk with its outer radius is

$$\text{Re} = \rho \frac{R_o v}{\mu_{\text{air}}} = \frac{2\pi N_m \rho R_o^2}{\mu_{\text{air}}}. \quad (10)$$

It is seen rotational (mechanical) loss is not relation to back iron.

- Stator winding loss will be obtained by the simple equation:

$$P_{\text{cu}} = R_s \times |I_{\text{load}}|^2. \quad (11)$$

- High frequency content of magnetic field causes additional loss (eddy current loss) in the stator winding [19]:

$$P_{\text{eddy_cu}} = \frac{(B_g \times 2 \times \pi \times f \times D_{\text{strand}} \times 10^{-3})^2}{32 \times \rho_{\text{cu}}} \times V_{\text{cu}}. \quad (12)$$

Simulation

Linking all subsystems of HSAFG model in a Matlab/Simulink environment, the computer model of the machine is obtained.

Simulation machine is a 30 kW, 400 Volts and 30000 rpm axial flux generator with two stators and three rotors.

An increment of thickness of back iron from 1 to 10

millimeters yields to reductions of the back-iron flux density (Fig. 4) and significant increase of the air-gap flux density (Fig. 5) for all numbers of pole. Air gap flux density configures the induce voltage and as seen in Fig. 6. As a conclusion, for providing sufficient voltage it is vital that the thickness of back iron for this machine be at least 3 millimeters.

According to the formula given in the previous section, mechanical loss (windage loss) is not related to L_{bi} and it is 3,286W for the simulation machine. Therefore, total power loss (Fig. 7) is depended on the copper and eddy current losses, so the power loss is increased. However output power (Fig. 8) is increased whilst the efficiency (Fig. 9) is changed accordingly by back iron variations. All these figures and discussion indicate that the thickness of back-iron is a vital parameter in the axial flux machine and its optimum value can be determined individually by full simulation of the machine.

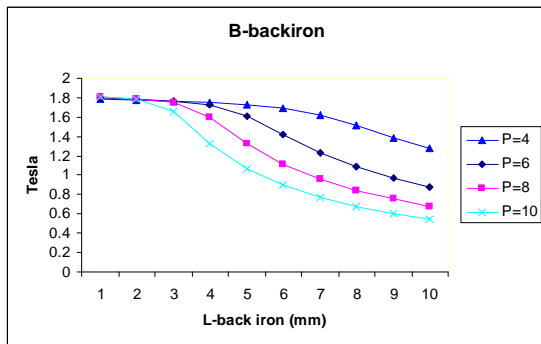


Fig. 4. Back-iron flux densities versus thickness of back iron

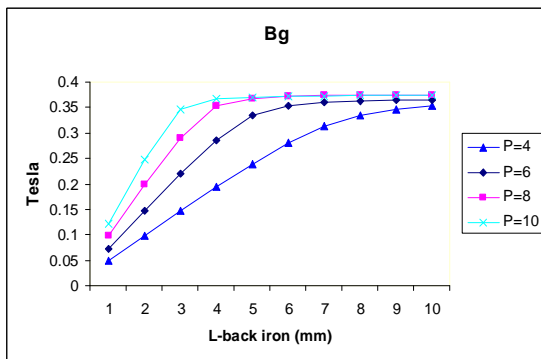


Fig. 5. Air gap flux densities versus thickness of back iron

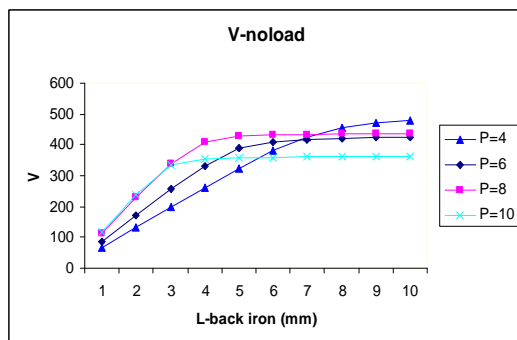


Fig. 6. Output voltage versus thickness of back iron

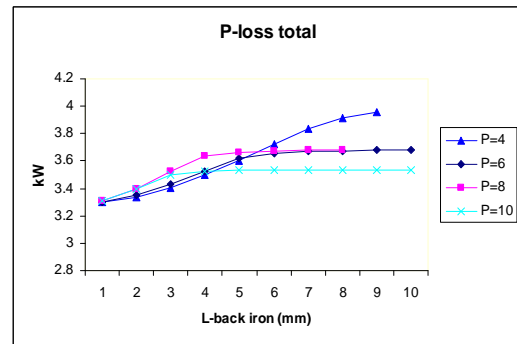


Fig. 7. Total power loss and output power versus thickness of back iron

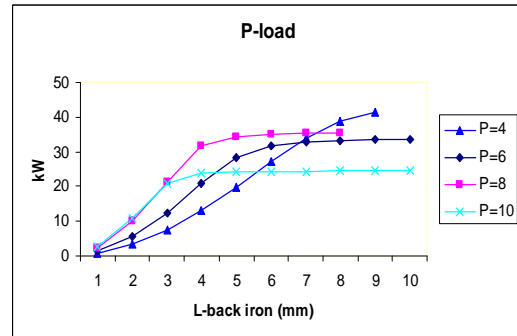


Fig. 8. Output power versus thickness of back iron

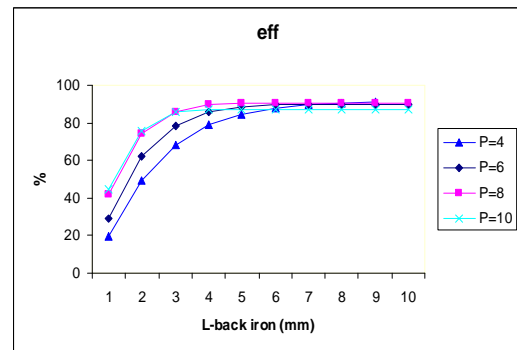


Fig. 9. Efficiency versus thickness of back iron

Conclusion

Modeling of a modular high-speed axial-flux PM generator were discussed in this paper.

For a given size and output power of the machine, the air gap flux is strictly related to the thickness of back-iron. Therefore, for producing sufficient air gap flux and resultant terminal voltage, adequate thickness of the rotor back-iron would be obligatory. Mass of the rotation parts including back-iron and cost of the machine are the main restrictions of an excessive large value of the back iron. Simulation of the machine with some details, would recommend an optimized values of the back-iron for a wide range of the output powers. For a given example machine it was illustrated, that an insufficient value of thickness of the rotor back iron reduces somewhat the terminal voltage and efficiency. Inversely if a large value of thickness is chosen the rotor inertia will increase and this may cause some mechanical problems with no significant improvement of the machine performance characteristics.

References

1. **Luk P. C. K., El-Hasan T. S.** Integrated design for a high speed permanent magnet axial flux generator // Magnetics Conference INTERMAG Asia 2005. – April 4–8, 2005. – P. 1083–1084.
2. **Wang Fengxiang, Zheng Wenpeng, Zong Ming, Wang Baoguo.** Design considerations of high-speed PM generators for micro turbines // International Conference on Power System Technology 2002. – Oct. 13–17, 2002. – Vol. 1. – P. 158–162.
3. **Brenard F. Kolanowski.** Guide to Microturbines. – The Fairmont Press. – 2004.
4. **Hamilton Stephanie L.** Microturbine Generator Handbook. – Pennwell Corporations. – 2003.
5. **Holmes A. S., Guodong Hong, Pullen K. R.** Axial-flux permanent magnet machines for micropower generation // Journal of Microelectromechanical Systems. – Feb. 2005. – Vol. 14, No. 1. – P. 54–62.
6. **Fengxiang Wang, Ming Zong, Wenpeng Zheng, Enlu Guan.** Design features of high speed PM machines // Sixth International Conference on Electrical Machines and Systems ICEMS 2003. – Nov. 9–11, 2003. – Vol. 1 – P. 66–70.
7. **Parviainen A., Pyrhonen J., Niemels M., Mantere J.** Performance Comparison between Low-Speed Axial-Flux and Radial-Flux Permanent-Magnet Machines Including Mechanical Constraints // IEEE International Conference on Electric Machines and Drives. – May 15, 2005. – P. 1695–1702.
8. **Sundaram K. B., Vaidya J., Zhao L., Acharya D., Ham C. H., Kapat J., Chow L.** Analysis and Test of a High-Speed Axial flux permanent magnet Synchronous motor // IEEE International Conference on Electric Machines and Drives. – May 15, 2005. – P. 119–124.
9. **Luk P. C., El-Hasan T.** Back iron design for high speed PM axial flux generators // IEEE International Magnetics Conference INTERMAG 2003. – March 28 – April 3, 2003. – P. HB–01.
10. **Aglen O.** Back-to-back tests of a high-speed generator // IEEE International Electric Machines and Drives Conference IEMDC'03. – June 1–4, 2003. – Vol. 2. – P. 1084–1090.
11. **Gieras J. F., Wang R. J., Kamper M. J.** Axial Flux Permanent Magnet Brushless machine. – Kluwer Academic Publisher. – 2005.
12. **El-Hassan T., Luk P. C.** Magnet topology optimization to reduce harmonics in high speed axial flux generators // IEEE International Magnetics Conference INTERMAG 2003. – March 28 – April 3, 2003. – P. GS–03.
13. **Hill-Cottingham R. J., Coles P. C., Eastham J. F., Profumo F., Tenconi A., Gianolio G., Cerchio M.** Plastic structure multi-disc axial flux PM motor // 37th IAS Annual Meeting Industry Applications Conference 2002. – Oct. 13–18, 2002. – Vol. 2. – P. 1274–1280.
14. **Chen Y., Pillay P.** Axial-flux PM wind generator with a soft magnetic composite core // Fourtieth IAS Annual Meeting Industry Applications Conference 2005. – Oct. 2–6, 2005. – Vol. 1. – P. 231–237.
15. **Rong-Jie Wang, Kamper M. J., Van der Westhuizen K., Gieras J. F.** Optimal design of a coreless stator axial flux permanent-magnet generator // IEEE Transactions on Magnetics. – Jan. 2005. Vol. 41, No. 1, Part 1. – P. 55–64.
16. **Lombard N. F., Kamper M. J.** Analysis and performance of an ironless stator axial flux PM machine // IEEE Transactions on Energy Conversion. – Dec. 1999. – Vol. 14, No. 4. – P. 1051–1056.
17. **Sadeghierad M., Lesani H., Monsef H., Darabi A.** Design considerations of High Speed Axial Flux permanent-magnet Generator with Coreless Stator // 8th IEEE International Power Engineering Conference IPEC 2007.
18. **Gieras J. F., Wang R. J., Kamper M. J.** Axial Flux Permanent Magnet Brushless machine. – Kluwer Academic Publisher. – 2005.
19. **Luk P. C. K., El-Hasan T. S.** Integrated design for a high speed permanent magnet axial flux generator // Magnetics Conference INTERMAG. – April 4–8, 2005. – P. 1083–1084.

Received 2008 10 31

M. Sadeghierad, H. Lesani, H. Monsef, A. Darabi. Back-iron Consideration in High-Speed Axial-Flux Machine // *Electronics and Electrical Engineering*. – Kaunas: Technologija, 2009. – No. 1(89). – P. 87–90.

High-Speed Axial Flux Generator (HSAFG) has come into attention because of its some advantages such as high power density and efficiency. This paper presents a modeling and designing procedure of HSAFG with some details. The optimized thickness of the back-iron used in the rotor of two ends is determined for a HSAFG by carefully considerations of the terminal voltage, output power and efficiency. It is illustrated that a very small thickness of the rotor yoke reduces the terminal voltage and efficiency and a very large value of it increases the rotor inertia, mechanical problems and cost of the machine with no significant improvement of the machine performance characteristics. Ill. 9, bibl. 19 (in English; summaries in English, Russian and Lithuanian).

M. Садегерад, Г. Лесани, Г. Монсеф, А. Дараби. Анализ ротора в быстродействующем генераторе осевого магнитного потока // *Электроника и электротехника*. – Каунас: Технология, 2009. – № 1(89). – С. 87–90.

Быстродействующий генератор осевого потока (HSAFG) популярен своими преимуществами, такими как высокая плотность мощности и эффективность. Представляется процедура моделирования и проектирования HSAFG. Конструкция ротора для HSAFG определена тщательно рассматривая предельное входное напряжение, выходную мощность и эффективность. Показано, что очень маленькая толщина хомута ротора уменьшает предельное напряжение и эффективность, а очень большая увеличивает инерцию ротора, механические проблемы и цену машины без существенного усовершенствования характеристик работы. Ил. 9, библи. 19 (на английском языке; рефераты на английском, русском и литовском яз.).

M. Sadeghierad, H. Lesani, H. Monsef, A. Darabi. Didelio greičio ašinio srauto generatoriaus rotorius analizė // *Elektronika ir elektrotechnika*. – Kaunas: Technologija, 2009. – Nr. 1(89). – P. 87–90.

Didelio greičio ašinio srauto generatorius (HSAFG) sulaukia dėmesio dėl tam tikrų savo pranašumų, tokių kaip didelis galios tankis ir efektyvumas. Pristatyta HSAFG modeliavimo ir projektavimo procedūra. Optimizuojant rotorius konstrukciją įvertinama įėjimo įtampa, išėjimo galia ir efektyvumas. Parodyta, kad labai mažas rotorius jungo storis sumažina gnybtų įtampą ir efektyvumą, o labai didelis storis didina rotorius inerciją, sukelia mechaninių problemų ir didina įrenginio kainą, bet jo našumo charakteristikos nepagerėja. Il. 9, bibl. 19 (anglų kalba; santraukos anglų, rusų ir lietuvių k.).

DOI: 10.5755/j02.eie.10583